Available online at www.sciencedirect.com

ScienceDirect

Procedia Structural Integrity 17 (2019) 900–905

Structural Integrity Procedia

www.elsevier.com/locate/procedia

ICSI 2019 The 3rd International Conference on Structural Integrity

High strain rate compressive behaviour of wood on the transverse plane

F. Gomes[a], J. Xavier[b]*, H. Koerber[c]

[a]*Universidade de Trás-os-Montes e Alto Douro, CITAB, Vila Real, 5001-801, Portugal*
[b] *UNIDEMI, Department of Mechanical and Industrial Engineering, Faculty of Sciences and Technology, Universidade NOVA de Lisboa, Caparica 2928-516, Portugal*
[c]*Technical University of Munich, Department of Mechanical Engineering, Chair for Carbon Composites, Boltzmannstraße 15, Garching, 85748, Germany*

Abstract

The high strain rate compressive behaviour of *Pinus pinaster* Ait. wood along the radial and tangential material axes was addressed in this work. Both quasi-static and dynamic tests were considered for comparation purposes. The quasi-static compression tests were performed on rectangular prismatic specimens along the radial and tangential directions coupled with digital image correlation. The high strain rate tests were carried out using a classical split-Hopkinson pressure bar coupled with a high-speed imaging system allowing independent kinematic measurements through digital image correlation. From these tests and material symmetry orientations, the constitutive curves were determined from which the Young modulus, Poisson's ratio and yield stress were evaluated and compared over the two different regimes over the strain rate spectrum. The mechanical properties observed for this species under quasi-static compression loading agree with reference values. A qualitative comparison between quasi-static and high strain rate regimes reveals a significant increase of some mechanical properties by increasing the strain rate. Quantitatively, by comparing mean values at the two strain rates, it was found that, in the radial direction, the modulus of elasticity increased by 6.3%, the yield stress showed an increase of 130.3% and the Poisson's ratio is slightly higher by 3.0%. Furthermore, in the tangential direction, it was found that the modulus of elasticity increased by 21.9% while the value of the yield stress showed an increase of 111.8%, and finally the Poisson's ratio presented a reduction of 24.3%.

Peer-review under responsibility of the ICSI 2019 organizers.

Keywords: high strain rate; wood

* Corresponding author. Tel.: +0-000-000-0000 ; fax: +0-000-000-0000 .
E-mail address: jmc.xavier@fct.unl.pt

2452-3216
Peer-review under responsibility of the ICSI 2019 organizers.
10.1016/j.prostr.2019.08.120

1. Introduction

Engineering materials are modelled by constitutive laws that describe their mechanical behaviour when subjected to the action of external forces. These constitutive models are of vital importance in computer-aided engineering systems. The material parameters included in these mathematical models must be determined experimentally for each material and considering several loading scenarios, which may cover a spectrum ranging viscoelasticity, quasi-static and dynamic (moderate and high) strain rates (Sharpe, 2008).

In recent times, due to an increased environmental awareness, there has been a general concern for the use of bio-based, renewable and sustainable materials in the most varied of applications (Thelandersson and Larsen, 2003). In this framework, this class of biological-based materials emerge as choice with great advantages over more traditional building materials over the light of several criteria (Börjesson and Gustavsson, 2000). Accordingly, wood and wood-based products are currently emerging as engineering materials sustained by the principle of circular economy. Current applications include loading scenarios whose mechanical behaviour can be described over a spectrum of strain regimes (Gilbertson and Bulleit, 2013). The understanding of the mechanical properties of wood over the different strain rate regimes is of extreme relevance for their applicability in new engineering solutions. However, considering wood as an anisotropic and heterogeneous material, the experimental characterisation of this material encompasses several challenges.

In moderate and high strain rate regimes, there is a few experimental set-ups that can be used for measuring the mechanical behaviour of materials (Field et al 2004). Among them, the split-Hopkinson pressure bar (SHPB) is the gold standard (Pankow, Attard, and Waas, 2009, Jacques et al., 2014, Koerber el al 2015). This test has been applied to address the dynamic behaviour of wood (Bragov and Lomunov, 1997, Allazadeh and Wosu, 2012, Gilbertson and Bulleit, 2013, Widehammar, 2002, 2004). Different purposes and goals were pursuit, the influence of moisture in the mechanical proprieties obtained using the SHPB, and the effect of load duration with regard to strain rate. From these previous works it can be concluded that it is expectable that the mechanical proprieties of wood species will increase by increasing the strain rate. However, as stated by Polocoşer, Kasal, Stöckel (2017), there is not a consensus about the pattern variation of some mechanical proprieties, primarily due to the absence of reliable data.

This work addresses the compression behaviour of *Pinus pinaster* Ait. wood in the transverse (radia-tangential) plane at quasi-static and high strain rate regimes. The SHPB was used for the high strain rate testing coupled with digital image correlation technique for the strain field reconstruction (Koeber, Xavier and Camanho, 2010). For comparative purposes quasi-static compression tests were also carried out on matched specimens.

2. Methods

2.1. Material and specimens

The wood material tested in this work was *Pinus pinaster* Ait. Matched specimens (*i.e.* in a close location within the stem to avoid natural variability among samples) were manufactured with nominal dimensions of 20×10×10 mm^3. For statistical representativeness, ten specimens per configuration were tested. Two different orientations were analysed by cutting the rectangular prismatic samples along the radial (0º) and tangential (90º) material symmetry directions.

2.2. Quasi-static tests

Compression tests were carried out in a universal MicroTester machine (model 5848, Instron, Barcelona, Spain). The load was measured by a cell with capacity of 2 kN. Tests were carried out under displacement control by setting the cross-head velocity to 0.2 mm/min. A loading cycle up to about 50 N was pre-applied before testing in order to accommodate the compression surfaces of the specimens to the testing machine platens.

The frontal surface of the specimens was painted to allow deformation measurements by the digital image correlation technique. A background matt white paint was firstly applied after surface polishing and cleaning. A

speckled pattern was then transferred using an airbrush (IWATA, model CM-B, Anesta Iwata Iberica SL, Barcelona, Spain) with matt black painting. The final random pattern was achieved with suitable contrast and speckle size in order to avoid both aliasing effects or low spatial resolution.

The digital image correlation technique was used to measure the strain field over the entire region of interest of the specimens. A coupled-charge device (CCD) camera (model Manta G-505, Allied Vision, Stadtroda, Germany) coupled with a lens (model AF Micro-Nikkor 200mm *f*/4D IF-ED) was used for image formation and acquisition. The MatchID software was used for DIC measurements (MatchID). The performance analysis tool was set-up to carry out a convergence study allowing a more deliberate choice of the DIC settings parameters (Pereira et al, 2018). Table 1 summarises the selected DIC parameters for this study.

Table 1. DIC setting parameters.

Correlation and strain derivation items	
Correlation criterion	ZNSSD
Image interpolation	Bicubic Spline
Shape function	Affine
Subset size	21×21 (0º specimen) | 31×31 (90º specimen)
Subset step	10 (0º specimen) 15 (90º specimen)
Strain window	9
Strain interpolation	Q4
Strain convention	Green-Lagrange

2.3. High-strain rate tests

High strain rate tests were carried out using the classical split-Hopkinson pressure bar. The striker-, incident- and transmission-bar were made of steel with a length 0.6, 2.6 and 1.3 m, respectively. The strain gauge on the incident-bar was located at 1.3 m, whilst they were at a distance of 0.3 m on the transmission-bar measured from the bar/specimen interface. The diameter of the bars was set-up with regard to the wooden specimen dimensions. Friction effects were minimized by applying a thin layer of MoS2 paste in between the bar end-faces and the specimen. For the determination of the in-plane strain fields across the region of interest of the specimen, the DIC technique was used. Images were recorded by a single Photron FASTCAM SA-5 high speed camera. The MatchID software was then used for further deformation processing. The high-speed camera was set to a frame rate of 100,000 fps with a corresponding pixel resolution of 320×192 pixel^2. To data synchronization between signals from the strain gauge on the bars and the optical measurements was achieved by trigging the camera automatically using an additional strain gauge mounted on the incident-bar.

3. Results

3.1. Quasi-static tests

From the raw data collected in the compression tests, the stress-strains curves were reconstructed as shown in Fig. 1 for both 0º and 90º specimen orientations, respectively. The constitutive curves show a dispersion within the natural variability of the material. The modulus of elasticity and Poisson's ratio were determined from these curves using least-square regression in the linear elastic domain. The yield stress was also measured from both specimen configurations, even though the tests were stopped at a given loading stage due to the significant out-of-plane localised damage, invalidating measurements on the densification region of the compression test of the cellular tissue (Miksic et al., 2013). On the one hand, the yielding of the radial (0º) specimens is rather driven by the buckling of earlywood cells due to the series arrangement of the annual rings. On the other hand, the yielding of the

tangential (90º) specimens is governed by the buckling of latewood layer on the parallel arrangement of the annual rings with regard to the load direction. Table 2 summarises the measured mechanical properties for the tested specimens in quasi-static compression tests.

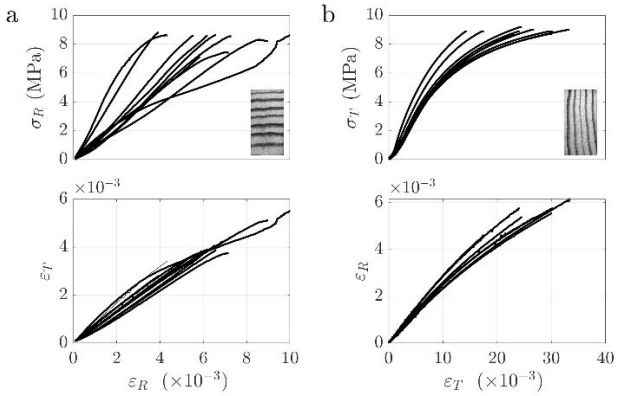

Fig. 1. $\sigma_i - \varepsilon_i$ (i=R,T) and $\varepsilon_j - \varepsilon_i$ (i,j=R,T) curves for: (a) 0º specimens; (b) 90º specimens.

Table 2-Mechanical proprieties obtained for the quasi-static regime

	E_R (GPa)	$\sigma_{y,0}$ (MPa)	ν_{RT}	E_T (GPa)	$\sigma_{y,90}$ (MPa)	ν_{TR}
Mean	1.561	7.621	0.673	0.772	3.834	0.281
Maximum	2.311	8.633	0.808	0.969	4.547	0.314
Minimum	1.079	4.7675	0.586	0.672	2.864	0.249
Standard deviation	0.363	1.191	0.071	0.097	0.455	0.023
COV (%)	23.3	15.6	10.5	12.5	11.9	8.4

3.2. High-strain rate tests

The data reduction of the SHPB can be designed either from the classical analysis (SHPBA), based on the strain signals from the bars, or integrating the strains measured directly on the specimen by means of the DIC measurements. Fig 2 shows the results for the tested specimens by both approaches. As it can be concluded, both analyses give equivalent material behaviours. However, the advantages of the second approach, by coupling SHPBA with DIC, can be highlighted from different perspectives (Koerber, Xavier and Camanho, 2010). Here it is just pointed out the fact that it allowed the measurement of the Poisson's ratio in the high strain rate regime. From these curves, mechanical properties of the wood species were determined. Table 3 and Table 4 summarise these results for both SHPBA only and SHPBA coupled with DIC. It can be seen that mean values are statistically equivalent, although for the E_R parameters a lower evaluation is obtained when using the axial strain based on DIC measurements.

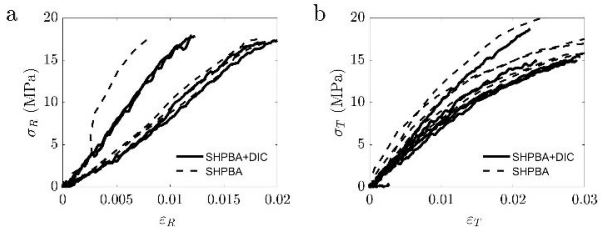

Fig. 2. Stress-strain curves referring to the use of the classical SHPB analysis (SHPBA) and integrating the SHPBA with DIC for: (a) 0º specimens; (b) 90º specimens.

Table 3-Mechanical proprieties obtained from the SHPBA.

	E_R (GPa)	$\sigma_{y,0}$ (MPa)	E_T (GPa)	$\sigma_{y,90}$ (MPa)
Mean	1.660	17.55	0.942	8.12
Maximum	1.794	17.92	1.103	10.60
Minimum	1.467	17.05	0.840	6.85
Standard deviation	0.327	0.390	0.106	1.448
COV (%)	8.3	2.2	11.2	17.8

Table 4-Mechanical proprieties obtained from the SHPBA and DIC.

	E_R (GPa)	$\sigma_{y,0}$ (MPa)	ν_{RT}	E_T (GPa)	$\sigma_{y,90}$ (MPa)	ν_{TR}
Mean	1.292	17.540	0.694	0.968	8.051	0.212
Maximum	1.477	17.926	0.744	1.292	10.403	0.247
Minimum	1.118	17.039	0.620	0.814	6.448	0.192
Standard deviation	0.175	0.453	0.056	0.192	1.683	0.024
COV (%)	13.6	2.6	8.14	0.192	20.9	11.3

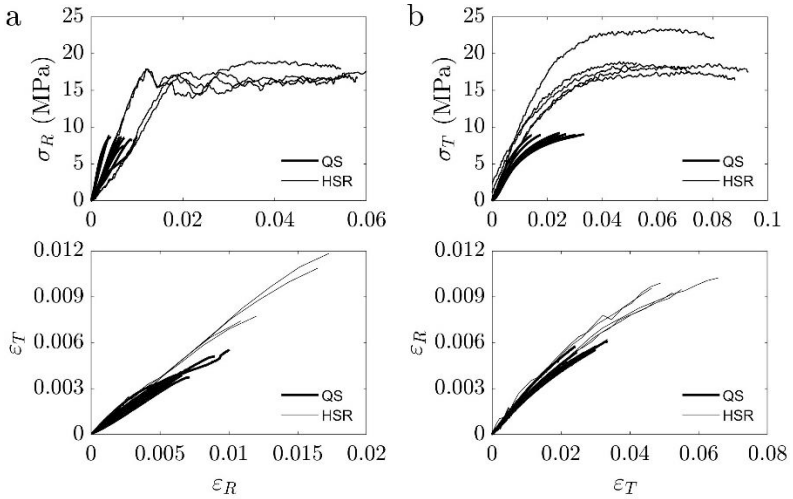

Fig. 3. $\sigma_R - \varepsilon_R$ and $\varepsilon_R - \varepsilon_T$ curves at both quasi-static and dynamic regimes for: (a) 0º specimens; (b) 90º specimens.

4. Discussion

In order to discuss the evolution of the mechanical parameters of the *P. pinaster* wood with regard to the strain rate regime, a qualitative comparison of the stress-strains curves is shown in Fig. 3. From this analysis, it is interesting to observe that, in general, the increase of the strain rate loading is accompanied by an increase of the stress-strain behaviour of the material. This is particularly true for the yield stress. It is verifiable that the value of the mechanical properties under analysis, namely the yield stress increased from quasi-static to high strain rate regimes. This observation is in line with conclusions obtained by Gilbertson and Bulleit (2013) and Widehammar (2004) who found that there is a significant increase in the mechanical properties of wood species due to the variation of the strain rates.

5. Conclusions

The compression behaviour of *Pinus pinaster* Ait. wood at quasi-static and high strain rate regimes was studied using two different specimen configurations, oriented, respectively, at the radial (0º) and tangential (90º) material directions. Both tests were coupled with digital image correlation technique for the strain field evaluation using standard and high-speed digital cameras for quasi-static and dynamic tests, respectively. Comparing mean values of mechanical properties from quasi-static to high strain rate regimes, it was observed that in the radial direction the modulus of elasticity increased by 6.3%, the yield stress increased by 130.3%, and the Poisson's ratio reduced by 10.6%. On the other hand, in the tangential direction, it was observed that the modulus of elasticity increased by 21.9%, the yield stress increased by 111.8%, whist the Poisson's ratio presents a reduction of 25.8%.

Acknowledgements

This work is supported by FCT - Portuguese Foundation for Science and Technology, under the projects UID/EMS/00667/2019 and UID/AGR/04033/2013. Authors would like to thank Prof. João Luis Pereira, Instituto Politécnico de Viseu for his help in the specimen preparation.

References

Allazadeh, M. R., Wosu, S.N. (2012). High strain rate compressive tests on wood. Strain 48, 101–107.

Börjesson, P., Gustavsson, L. (2000). Greenhouse gas balances in building construction: Wood versus concrete from life-cycle and forest land-use perspectives. Energy Policy 28, 575–588.

Bragov, A., Lomunov, A. (1997). Dynamic properties of some wood species. Le Journal de Physique IV, 7(3, Supplément), C3-487-C3-492.

Field, J. E., Walley, S. M., Proud, W. G., Goldrein, H. T., Siviour, C. R. (2004). Review of experimental techniques for high rate deformation and shock studies. International Journal of Impact Engineering 30, 725–775.

Gilbertson, C. G., Bulleit, W. M. (2013). Load duration effects in wood at high strain rates. Journal of Materials in Civil Engineering 25, 1647–1654.

Jacques, E., Lloyd, A., Braimah, A., Saatcioglu, M., Doudak, G., Abdelalim, O. (2014). Influence of high strain-rates on the dynamic flexural material properties of spruce–pine–fir wood studs. Canadian Journal of Civil Engineering 41, 56–64.

Koerber, H., Xavier, J., Camanho, P.P. (2010). High strain rate characterisation of unidirectional carbon-epoxy IM7-8552 in transverse compression and in-plane shear using digital image correlation. Mechanics of Materials 42, 1004-1019.

Koerber, H., Xavier, J., Camanho, P.P., Essa, Y.E., Martín de la Escalera, F. (2015). High strain rate behaviour of 5-harness-satin weave fabric carbon-epoxy composite under compression and combined compression-shear loading. International Journal of Solids and Structures 54, 172-182.

MatchID (2018). MatchID Manual. MatchID: Metrology beyond Colors.

Miksic, A. et al. (2013). Effect of fatigue and annual rings orientation on mechanical properties of wood under cross-grain uniaxial compression.
Wood Science and Technology 47, 1117–1133.

Pankow, M., Attard, C., Waas, A. M. (2009). Specimen size and shape effect in split Hopkinson pressure bar testing. Journal of Strain Analysis for Engineering Design 44, 689–698.

Pereira, J.L., Xavier, J., Ghiassi, B., Lousada, J., Morais, J. (2018). On the identification of earlywood and latewood radial elastic modulus of Pinus pinaster by digital image correlation: A parametric analysis. Journal of Strain Analysis for Engineering Design 53, 566–574.

Polocoşer, T., Kasal, B., Stöckel, F. (2017). State-of-the-art: intermediate and high strain rate testing of solid wood. Wood Science and Technology 51, 1479–1534.

Sharpe, W.N. (2008). Springer Handbook of Experimental Solid Mechanics, 929–959.

Thelandersson, S., Larsen, H.J. (2003). Timber Engineering. John Wiley & Sons.

Widehammar, S. (2002). A method for dispersive split Hopkinson pressure bar analysis applied to high strain rate testing of spruce wood. Uppsala University, Sweden.

Widehammar, S. (2004). Stress-strain relationships for spruce wood: Influence of strain rate, moisture content and loading direction. Experimental Mechanics, 44(1), 44–48.